

Immobilization of platinum(II) and palladium(II) complexes on metal oxides by sol–gel processing and surface modification using bifunctional phosphine–phosphonate esters

Gilles Guerrero,^a P. Hubert Mutin,^{*a} E. Framery^b and André Vioux^a

Received (in Montpellier, France) 7th January 2008, Accepted 4th April 2008

First published as an Advance Article on the web 7th May 2008

DOI: 10.1039/b800250a

The bifunctional phosphine–phosphonate ester derivatives $\text{Ph}_2\text{P}(\text{CH}_2)_3\text{P}(\text{O})(\text{OSiMe}_3)_2$ (**L**), (*cis*- $\text{Cl}_2\text{Pt}[\text{Ph}_2\text{P}(\text{CH}_2)_3\text{P}(\text{O})(\text{OSiMe}_3)_2]_2$) (**1**), *trans*- $\text{Cl}_2\text{Pd}[\text{Ph}_2\text{P}(\text{C}_6\text{H}_4)\text{P}(\text{O})(\text{OSiMe}_3)_2]_2$ (**2**) and *trans*- $\text{Cl}_2\text{Pd}[\text{Ph}_2\text{P}(\text{C}_6\text{H}_4)\text{P}(\text{O})(\text{OEt})_2]_2$ (**3**) were used to immobilize platinum(II) and palladium(II) complexes on metal oxide supports by three different routes: sol–gel incorporation of **L** in TiO_2 or ZrO_2 matrices followed by complexation with $\text{PtCl}_2(\text{PhCN})_2$, direct sol–gel immobilization of **1** and **2**, surface modification of TiO_2 nanoparticles with **2** and **3**. The hybrid solids were characterized by solid-state ^{31}P MAS NMR spectroscopy, surface area measurements and chemical analysis; the advantages and disadvantages of the different routes were discussed. This study demonstrates that phosphonic esters can provide a valuable alternative to phosphonic acids for the preparation of functional organic–inorganic hybrids based on metal oxides.

Introduction

Phosphonic acids, RPO_3H_2 , are attracting increasing interest as anchoring groups for the synthesis of hybrid organic–inorganic materials, either by sol–gel processing or surface modification.¹ Indeed, phosphonic acids bind to a wide range of metal oxides.^{2–5} The anchoring results from the formation of stable M–O–P bonds by condensation with surface hydroxyl groups and coordination of the phosphoryl oxygen with surface metal atoms.⁶ Thus, phosphonic acids have been used to immobilize transition metal complexes for application in photovoltaic cells,^{7–9} photoelectrochromic devices^{10,11} or catalysis.^{12,13}

The main limitations in the use of phosphonic acids as anchoring functions come from their reactivity that make them incompatible with acid-sensitive organic functions, and from their poor solubility in common organic solvents.

In most cases, the synthesis of phosphonic acids involves the preparation of diethyl phosphonate esters. In addition, as the hydrolysis of diethyl phosphonates requires harsh acidic conditions, they are usually converted into silylated phosphonates that can be hydrolyzed under very mild conditions. A few years ago, we showed that such phosphonate ester intermediates ($\text{PhPO}(\text{OSiMe}_3)_2$ and $\text{PhPO}(\text{OEt})_2$) could be used directly as anchoring functions on TiO_2 or Al_2O_3 .^{2,3}

In the present work we report the successful immobilization of phosphine ligands and Pt or Pd complexes on TiO_2 or ZrO_2

using bifunctional phosphine–phosphonate esters instead of acids, as depicted in Scheme 1. Characterization of the hybrid solids by solid-state MAS NMR spectroscopy and elemental analysis showed that the use of phosphonate esters permit the avoidance of the formation of phosphonium species by reaction of the acidic POH groups with the phosphine ligands; phosphonium are poor ligands, which would influence the formation and stability of Pt or Pd complexes.^{14,15} In addition, phosphonate esters are easier to synthesize than the acids and are easily soluble in common organic solvents. This study demonstrates that phosphonic esters can provide distinct advantages over phosphonic acids for the preparation of functional hybrid materials, particularly in the case of acid-sensitive functions.

Experimental

Chemicals

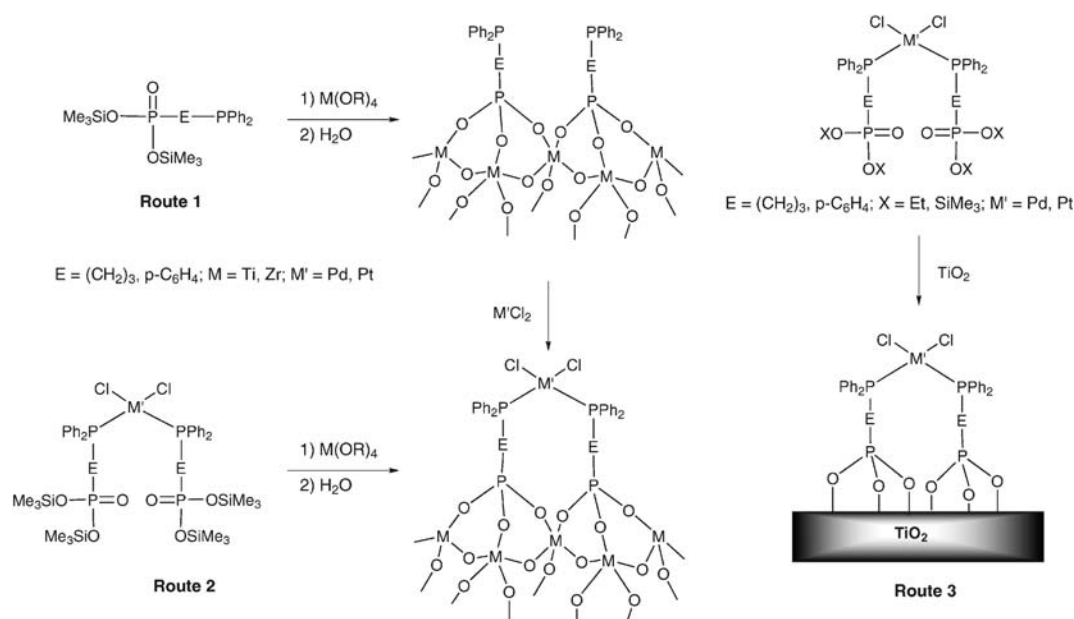
All manipulations were carried out under an atmosphere of dry argon using standard Schlenk and glovebox techniques. Solvents were dried by conventional procedures before use. $\text{Ti}(\text{O}^i\text{Pr})_4$ (97%) was distilled prior to use. $\text{Zr}(\text{O}^i\text{Pr})_4 \cdot i\text{PrOH}$ (99.9%), Me_3SiBr and water (HPLC grade) were purchased from Aldrich and used as received. TiO_2 P25 (70% anatase, average particle size 21 nm, specific surface area $50 \text{ m}^2 \text{ g}^{-1}$) graciously provided by the Degussa company, was dried before use (12 h, 120°C , $5 \times 10^{-2} \text{ mbar}$).

Synthesis of the precursors

The precursors used in this study are presented in Table 1. The diethyl phosphonated–phosphine ligands $\text{Ph}_2\text{P}(\text{CH}_2)_3\text{PO}(\text{OEt})_2$ and $\text{Ph}_2\text{PC}_6\text{H}_4\text{PO}(\text{OEt})_2$ were prepared by conventional procedures^{16–19} and were used for the synthesis of complexes *cis*- $\text{Cl}_2\text{Pt}[\text{Ph}_2\text{P}(\text{CH}_2)_3\text{PO}(\text{OEt})_2]_2$ and *trans*- $\text{Cl}_2\text{Pd}[\text{Ph}_2\text{P}(\text{C}_6\text{H}_4)\text{PO}(\text{OEt})_2]_2$ (**3**) as described in a previous

^a Institut Charles Gerhardt, équipe CMOS, UMR CNRS 5253, Université Montpellier 2, CC 1701, Place E. Bataillon, 34095 Montpellier cedex 5, France. E-mail: guerrero@univ-montp2.fr; Fax: 334 6714 3852; Tel: 334 6714 3802

^b Institut de Chimie et Biochimie Moléculaires et Supramoléculaires, équipe SASYM, UMR CNRS 5246, Université Claude Bernard Lyon 1, Domaine scientifique de la Doua, Bât. CPE (Curien 308), 43 Boulevard du 11 novembre 1918, 69622 Villeurbanne cedex, France. Fax: 334 7244 8160; Tel: 334 7244 6263



Scheme 1 Immobilization of phosphine-phosphonate ligands and metal complexes by sol-gel routes (routes 1 and 2) and surface modification (route 3).

article.²⁰ The trimethylsilylated phosphonate precursors $\text{Ph}_2\text{P}(\text{CH}_2)_3\text{PO}(\text{OSiMe}_3)_2$ (**L**), *cis*- $\text{Cl}_2\text{Pt}[\text{Ph}_2\text{P}(\text{CH}_2)_3\text{PO}(\text{OSiMe}_3)_2]_2$ (**1**), and *trans*- $\text{Cl}_2\text{Pd}[\text{Ph}_2\text{P}(\text{C}_6\text{H}_4)\text{PO}(\text{OSiMe}_3)_2]_2$ (**2**) were prepared from the corresponding ethyl esters, by reaction under argon with Me_3SiBr (3 eq. Me_3SiBr per diethyl phosphonate group) in dry CH_2Cl_2 at room temperature for 2 h, followed by removal of the volatiles under vacuum.²¹ It should be noted that the geometry of the complexes (*cis* or *trans*) was not modified by the silylation step as shown by solution ^{31}P NMR (Table 1).

Preparation of the xerogels

Metal oxide-based hybrid gels were prepared from metal isopropoxide and trimethylsilylated precursors in two steps (Table 2). In the first step, the metal alkoxide was added to a solution of the trimethylsilylated precursor in CH_2Cl_2 ($\text{M} = \text{Ti}$) or in THF ($\text{M} = \text{Zr}$), leading to clear solutions in all cases, with a metal alkoxide concentration of 0.8 mol L^{-1} . After stirring for 2 h at room temperature, a stoichiometric amount of water was added dropwise over a period of 1 h, leading to opaque gels.

Before analysis, the samples were aged at room temperature for 2 days, then washed successively with the reaction solvent, water, ethanol and diethyl ether. The final xerogels were obtained by drying under vacuum (10^{-1} mbar) at 120°C for 5 h.

Complexation of the xerogels

A fourfold molar excess of $\text{PtCl}_2(\text{PhCN})_2$ (with respect to a Pt/PPh_2 ratio of 0.5 for an expected monometallic complex) was added to the xerogel in suspension in dry dichloromethane. After refluxing for 24 h (40°C) under an argon atmosphere, the suspension was filtered, washed successively with dichloromethane and diethyl ether, then dried under vacuum (10^{-1} mbar) at 100°C for 5 h.

Surface modification of TiO_2

G1 was prepared by reaction of dried TiO_2 (1 g) with complex **1** (0.845 mmol) in dry dichloromethane (40 mL) under argon at room temperature for 24 h. The solid was then filtered off on a $0.45 \mu\text{m}$ Millipore membrane, washed successively with dichloromethane, water, ethanol and diethyl ether, then dried under vacuum at 120°C for 5 h. **G2** was prepared by a similar procedure but using complex **3** (0.831 mmol) and a reaction temperature of 40°C (Table 2).

Analytical methods

Solution ^{31}P NMR spectroscopy was performed using a Bruker DPX200 spectrometer. Solid-state ^{31}P NMR spectra were recorded on a Bruker Avance DPX300 spectrometer at 121.5 MHz , using magic angle spinning (MAS) (spinning rate 10 kHz) and high-power proton decoupling, with a 45° flip angle and a 10 to 40 s recycling

Table 1 Phosphonate precursors used in this study and their solution ^{31}P NMR chemical shifts

Precursor	$\delta(^{31}\text{P})/\text{ppm}$	Solvent
$\text{Ph}_2\text{P}(\text{CH}_2)_3\text{PO}(\text{OSiMe}_3)_2$ L	-15.7 (CPh_2); 26.7 (CPO_3Si_2)	$\text{CH}_2\text{Cl}_2\text{-CD}_3\text{COCD}_3$
<i>cis</i> - $\text{Cl}_2\text{Pt}[\text{Ph}_2\text{P}(\text{CH}_2)_3\text{PO}(\text{OSiMe}_3)_2]_2$ 1	7.7 (PtCPh_2); 25.4 (CPO_3Si_2)	$\text{CH}_2\text{Cl}_2\text{-CD}_3\text{COCD}_3$
<i>trans</i> - $\text{Cl}_2\text{Pd}[\text{Ph}_2\text{P}(\text{C}_6\text{H}_4)\text{PO}(\text{OSiMe}_3)_2]_2$ 2	23.8 (PdArPPh_2); 3.1 (ArPO_3Si_2)	$\text{CH}_2\text{Cl}_2\text{-CD}_3\text{COCD}_3$
<i>trans</i> - $\text{Cl}_2\text{Pd}[\text{Ph}_2\text{P}(\text{C}_6\text{H}_4)\text{PO}(\text{OEt})_2]_2$ 3	24.2 (PdArPPh_2); 17.9 (ArPO_3Et_2)	CDCl_3

Table 2 Nomenclature of hybrids obtained by sol–gel process or surface modification

Xerogel	Reaction
X1	4.25 Zr(OiPr) ₄ ·iPrOH + Ph ₂ P(CH ₂) ₃ PO(OSiMe ₃) ₂ (L) + 7.5 H ₂ O
X2	5 Ti(OiPr) ₄ + Ph ₂ P(CH ₂) ₃ PO(OSiMe ₃) ₂ (L) + 9 H ₂ O
X3	X1 + PtCl ₂ (PhCN) ₂
X4	X2 + PtCl ₂ (PhCN) ₂
X5	10 Zr(OiPr) ₄ ·iPrOH + <i>cis</i> -Cl ₂ Pt[Ph ₂ P(CH ₂) ₃ PO(OSiMe ₃) ₂] ₂ (1) + 18 H ₂ O
X6	10 Zr(OiPr) ₄ ·iPrOH + <i>trans</i> -Cl ₂ Pd[Ph ₂ P(C ₆ H ₄)PO(OSiMe ₃) ₂] ₂ (2) + 18 H ₂ O
X7	10 Ti(OiPr) ₄ + <i>trans</i> -Cl ₂ Pd[Ph ₂ P(C ₆ H ₄)PO(OSiMe ₃) ₂] ₂ (2) + 18 H ₂ O
Grafted titania	Reaction
G1	TiO ₂ + <i>cis</i> -Cl ₂ Pt[Ph ₂ P(CH ₂) ₃ PO(OSiMe ₃) ₂] ₂ (1)
G2	TiO ₂ + <i>trans</i> -Cl ₂ Pd[Ph ₂ P(C ₆ H ₄)PO(OEt) ₂] ₂ (3)

delay. ³¹P chemical shifts were referenced to H₃PO₄ (85% in water).

Elemental analyses were performed at the laboratory of microanalyses of the CNRS in Vernaison (France). The BET surface areas of the samples were obtained from nitrogen adsorption experiments at 77 K with a Micromeritics Gemini2360 sorptometer.

Results and discussion

In a previous publication, we described the synthesis of diethyl phosphonated phosphine ligands and their Pd(II) and Pt(II) complexes.²⁰ These compounds are used as starting compounds for the preparation of the precursors employed in this study (Table 1). The first part of this work presents the immobilization of phosphine groups or metal complexes by sol–gel processing, the second part describes the immobilization of metal complexes by surface modification of a titania support (Table 2, Scheme 1).

Sol–gel processing: routes 1 and 2

The xerogel samples (Table 2) have been prepared from bistrimethylsilyl esters and metal alkoxides precursors using a two-step sol–gel process studied in former publications.^{6,22,23} In this process, the first step involves the formation of P–O–M bonds (M = Zr, Ti) by non-hydrolytic condensation of P–O–SiMe₃ and M–OiPr groups and also by coordination of the P=O groups.

In the second step water is added to promote the formation of M–O–M bonds by classical hydrolysis–condensation of the remaining M–OiPr groups. As shown in Scheme 1 and Table 2, the sol–gel immobilization of metal complexes has been done in two different ways: immobilization of phosphine ligands in a gel followed by complexation (**X3**, **X4**) (route 1), or direct immobilization of the Pt or Pd complex in the gel (**X5**, **X6**) (route 2). Fig. 1 shows the ³¹P MAS NMR spectra of the phosphine ligand **L** (Ph₂P(CH₂)₃PO(OSiMe₃)₂) immobilized in a ZrO₂ matrix (**X1**) or in a TiO₂ matrix (**X2**). The spectrum of **X1** shows two resonances at –16.2 and 24.1 ppm, which can be unambiguously ascribed to the free phosphine functions (–(CH₂)₃PPh₂ sites) (Table 3, entry 1) and to the phosphonate groups bonded to the metal oxide matrix, respectively. These two resonances are in a 1 : 1 ratio showing that no secondary reaction such as phosphine oxidation or formation of a

phosphonium took place. The spectrum of **X2** is similar to that of **X1**, but the ratio between the resonances at –16.4 and 24.9 ppm is about 0.85 : 1.15. In addition, the signal centered at 24.9 ppm is broader and shows a shoulder at about 31 ppm. Simulation of the ³¹P NMR spectrum of **X2** (Table 4) confirmed the presence of an additional resonance at 30.8 ppm suggesting that about 15% of the phosphine groups were oxidized during the synthesis of the solid, leading to –(CH₂)₃-PPh₂(O) sites (Table 3, entries 2a and b).

The M/P ratios (M = Zr, Ti) derived from elemental analysis of xerogels **X1** and **X2** (Table 5) are very close to the calculated values, indicating in both cases quantitative incorporation of the phosphine–phosphonate ligands in the oxide matrix. The BET specific surface area of xerogels **X1** and **X2** are very low (<10 m² g^{–1}). Nevertheless, elemental

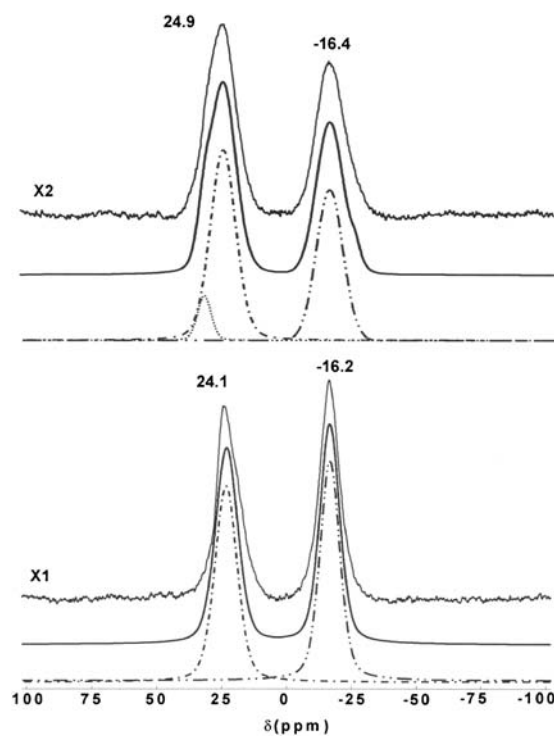


Fig. 1 Experimental and simulated (solid line) ³¹P MAS NMR spectra of xerogels **X1** (ZrO₂/Ph₂P(CH₂)₃PO₃) and **X2** (TiO₂/Ph₂P(CH₂)₃PO₃); PO₃ (---); PPh₂ (— · —); P(Ph₂)₂ (···).

Table 3 Solid-state and solution ^{31}P NMR chemical shifts of selected phosphine, phosphine oxide and phosphonium sites

Entry	Site	$\delta(^{31}\text{P})/\text{ppm}$	Ref.
1	$-(\text{CH}_2)_3\text{PPh}_2$	-16.3 (CP-MAS)	14
2a	$-(\text{CH}_2)_3\text{P}(\text{O})\text{Ph}_2$	28.6	24
2b	$-(\text{CH}_2)_3\text{P}(\text{O})\text{Ph}_2$	31.7	25
3	$-(\text{CH}_2)_3\text{HPh}_2\text{P}^+\text{Cl}^-$	5.8 (CP-MAS)	14
4	<i>cis</i> - $[(\text{CH}_2)_3\text{PPh}_2]_2\text{Pt}$	7.5 ^a	20
5	<i>trans</i> - $[(\text{CH}_2)_3\text{PPh}_2]_2\text{Pt}$	12.4 ^b	20
6	$-(\text{C}_6\text{H}_4)\text{PPh}_2$	-4.6	20
7a	$-(\text{C}_6\text{H}_4)\text{P}(\text{O})\text{Ph}_2$	29.8	26
7b	$-(\text{C}_6\text{H}_4)\text{P}(\text{O})\text{Ph}_2$	30.7 (CP-MAS)	26
8	<i>cis</i> - $[(\text{C}_6\text{H}_4)\text{PPh}_2]_2\text{Pd}$	32.6	27
9	<i>trans</i> - $[(\text{C}_6\text{H}_4)\text{PPh}_2]_2\text{Pd}$	23.8	20

^a Pseudo-triplet, $^1J_{\text{Pt-P}} = 3643 \text{ Hz}$. ^b Pseudo-triplet, $^1J_{\text{Pt-P}} = 2550 \text{ Hz}$.

analyses of **X3** and **X4** (obtained by reaction of **X1** and **X2** with $\text{PtCl}_2(\text{PhCN})_2$ in CH_2Cl_2) indicate that the Pt/P ratios are close to the value of 0.25 calculated assuming quantitative complexation of the phosphine functions and formation of monometallic complexes (Table 5). The near disappearance of the resonances corresponding to free phosphine sites in the ^{31}P MAS NMR spectra of xerogels **X3** and **X4** confirms the nearly complete complexation of the phosphine sites (Fig. 2). Both spectra display a major resonance centered at about 23 ppm, ascribed to the phosphonate groups bonded to the oxide matrix, and two additional signals centered at about 13 and 2 ppm. Comparison with ^{31}P NMR chemical shifts of Pt(II) complexes (Table 3, entries 4 and 5) suggests that the immobilized Pt complexes are mostly in a *trans* geometry.

Indeed, in such a geometry, the coupling of ^{31}P with ^{195}Pt ($I = 1/2$; 33.8%) would lead to satellite signals at 2.5 ppm and 23.5 ppm (for a central signal at 13 ppm). However, due to the lack of resolution of the different signals it is difficult to propose a reliable simulation, and the presence of *cis* sites (Table 3, entry 4) or phosphonium sites (arising from phosphine protonation) (Table 3, entry 3) cannot be discarded. On the other hand, the ^{31}P MAS NMR spectrum of **X5** prepared

by direct immobilization of complex **1** in a ZrO_2 matrix (route 2) is better resolved (Fig. 3) and can be easily simulated using a resonance at 22.9 ppm corresponding to phosphonate groups bonded to the oxide matrix, and a pseudo-triplet centered at 7.9 ppm with a coupling constant close to 3500 Hz characteristic of a monometallic Pt(II) complex in a *cis* geometry (Table 3, entry 4), as in the initial complex **1**. The ratio between the two sets of resonances is close to 1 (Table 4), indicating that no isomerization or secondary reactions such as decomplexation or oxidation of the phosphine groups occurred during the sol-gel incorporation of complex **1**. In addition, the absence of a sharp resonance at about 25 ppm corresponding to dangling $(\text{CH}_2)_n\text{PO}(\text{OH})_2$ groups^{28,29} that would arise from hydrolyzed but uncondensed $(\text{CH}_2)_n\text{PO}(\text{OSiMe}_3)_2$ groups, shows that the two phosphonate groups in complex **1** are linked to the oxide network, as illustrated in Scheme 1.

The Zr/P and Pt/P ratios given by the elemental analysis (Table 5) are close to the expected values, indicating a nearly quantitative incorporation of complex **1** in the solid and confirming the absence of decomplexation during the sol-gel process.

The Pd(II) complex **2** was also immobilized in a ZrO_2 and TiO_2 matrices by route 2. The ^{31}P NMR spectra of **X6** and **X7** show three main signals (Fig. 3). The signal at about 10 ppm may be attributed to phenylphosphonate groups bonded to zirconia or titania.²² The resonance at about 22 ppm is ascribed to phosphine sites in a *trans* geometry as in the initial complex **2** (Table 1 and Table 3, entry 9). A third signal centered at about 32 ppm is also present in both spectra. This chemical shift can correspond either to phosphine sites complexed to Pd(II) in a *cis* geometry (Table 3, entry 8), which would indicate significant isomerization of the Pd complex, or to phosphine oxide sites (Table 3, entries 7a and 7b), which would arise from the decomplexation of the Pd center and oxidation of the resulting free phosphine.

The Zr/P and Pd/P ratios determined by elemental analysis (Table 5) of **X6** and **X7** are close to the expected values, suggesting that complex **2** was incorporated in the oxide

Table 4 Parameters used for the simulation of the ^{31}P NMR spectra of the hybrid samples

Sample	Chemical shift, δ/ppm	Attribution	Integral (%)	$^1J_{\text{Pt-P}}/\text{Hz}$
X1	-16.7	PPh_2	51	—
	23.0	PO_3	49	—
X2	-16.6	PPh_2	42.5	—
	24.5	PO_3	50	—
	30.8	PPh_2O	7.5	—
X5	21.8	PO_3	50	—
	8.1; -6.6; 21.8	<i>cis</i> - PPh_2Pt	33; 8.5; 8.5	3452
X6	8.2	PO_3	50	—
	31.0	<i>cis</i> - PPh_2Pd and/or PPh_2O	23	—
	22.4	<i>trans</i> - PPh_2Pd	27	—
X7	11.1	PO_3	49	—
	33.4	<i>cis</i> - PPh_2Pd and/or PPh_2O	22	—
	22.5	<i>trans</i> - PPh_2Pd	29	—
G1	28.4	PO_3	49	—
	7.7; -5.6; 22.2	<i>cis</i> - PPh_2Pt	33; 9; 9	3377
G2	-4.1	PPh_2	4.5	—
	12.4	PO_3	48.5	—
	32.8	<i>cis</i> - PPh_2Pd and/or PPh_2O	16	—
	22.2	<i>trans</i> - PPh_2Pd	31	—

Table 5 M/P Ratios (derived from elemental analysis and calculated from the amount of reactants, assuming complete condensation and complexation) and complex loading of the xerogels

Xerogel	M/P (M = Ti, Zr)	M'/P (M' = Pd, Pt)	Loading (mmol complex/ mol oxide)
	Found (calc.)	Found (calc.)	
X1	2.0 (2.1)	—	—
X2	2.4 (2.5)	—	—
X3	2.6 (2.1)	0.23 (0.25)	95
X4	2.2 (2.5)	0.23 (0.25)	115
X5	2.8 (2.5)	0.22 (0.25)	90
X6	2.6 (2.5)	0.31 (0.25)	110
X7	2.9 (2.5)	0.29 (0.25)	86

matrices quantitatively and that no decomplexation took place, which is in favor of isomerization rather than decomplexation/oxidation. Furthermore, no signal corresponding to free phosphine sites are detected around -5 ppm (Table 3, entry 6) and it would be surprising to have complete oxidation of the phosphine sites formed by decomplexation whereas no oxidation of the free phosphine sites was detected for ZrO₂ matrices, as shown by the spectrum of X1 in Fig. 1. Thus, although decomplexation/oxidation cannot be ruled out on the grounds of chemical shifts only, the signal at about 32 ppm most likely corresponds to phosphine sites complexed to Pd(II) in a *cis* geometry.

The simulation of the spectra (Table 4) indicate that the resonance at about 10 ppm represents 50% of the phosphorus species, which is consistent with both assignments. As previously noted for X5, the absence of a sharp signal at about 15 ppm corresponding to uncondensed $-C_6H_4-PO(OH)_2$ groups³⁰ shows that the two phosphonate groups in complex 2 are linked to the zirconia matrix (Scheme 1).

Thus, using the sol-gel route 2, it is possible to immobilize directly metal complexes. In the case of the palladium complex

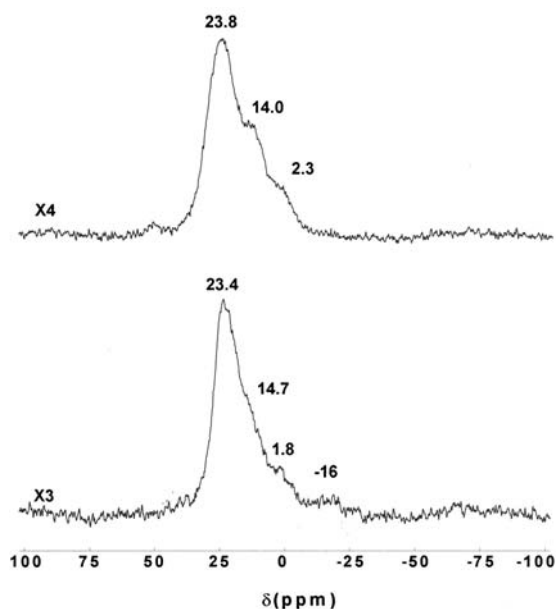


Fig. 2 Experimental ³¹P MAS NMR spectra of xerogels X3 (X1 + PtCl₂(PhCN)₂) and X4 (X2 + PtCl₂(PhCN)₂).

2, partial isomerization or decomplexation/oxidation of the phosphine groups occurred, whereas no such secondary reactions occurred for the platinum complex 1. However, only low surface-area xerogels ($S_{BET} < 10 \text{ m}^2 \text{ g}^{-1}$) have been obtained, which are not well-suited to applications such as heterogeneous catalysis. To avoid this problem, we investigated the surface modification of titania particles ($S_{BET} = 50 \text{ m}^2 \text{ g}^{-1}$) with different complexes (route 3).

Grafting of TiO₂ particles: route 3

The hybrid samples G1 and G2 have been prepared by direct surface modification of titania P25 nanoparticles using complexes 1 and 3, respectively (Table 2, Scheme 1). As discussed in previous publications, the grafting process likely involves the formation of P–O–M bonds by condensation of P–O–X (X

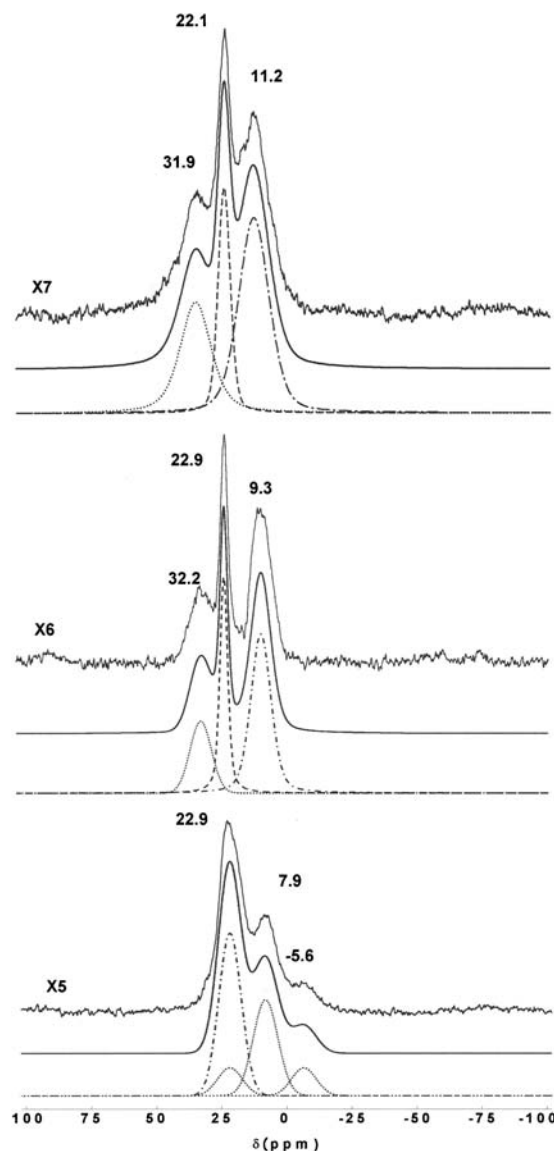


Fig. 3 Experimental and simulated (solid line) ³¹P MAS NMR spectra of xerogels X5 (ZrO₂/*cis*-Cl₂Pt[Ph₂P(CH₂)₃PO(OSiMe₃)₂]₂), X6 (ZrO₂/*trans*-Cl₂Pd[Ph₂P(C₆H₄)PO(OSiMe₃)₂]₂) and X7 (TiO₂/*trans*-Cl₂Pd[Ph₂P(C₆H₄)PO(OSiMe₃)₂]₂): PO₃ (---), *cis*-PPh₂M (···), *trans*-PPh₂M (--).

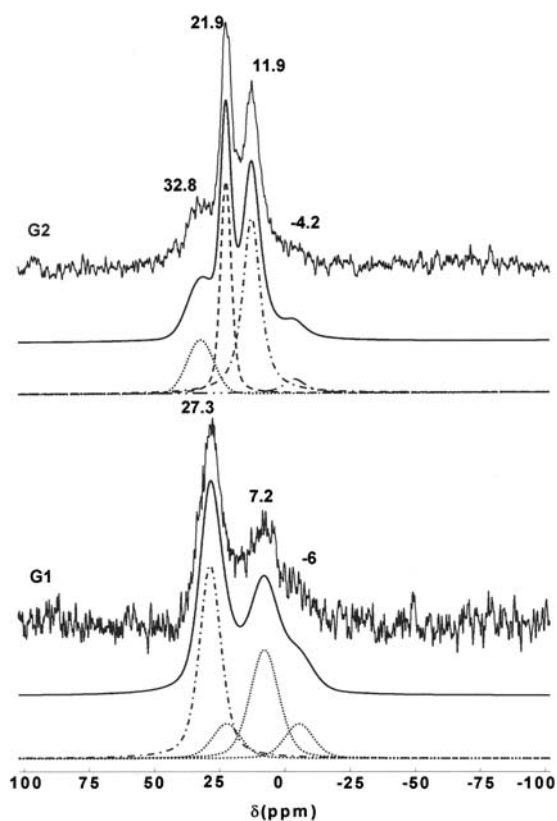


Fig. 4 Experimental and simulated (solid line) ^{31}P MAS NMR spectra of **G1** ($\text{TiO}_2 + \text{cis-Cl}_2\text{Pt}[\text{Ph}_2\text{P}(\text{CH}_2)_3\text{PO}(\text{OSiMe}_3)_2]_2$) and **G2** ($\text{TiO}_2 + \text{trans-Cl}_2\text{Pd}[\text{Ph}_2\text{P}(\text{C}_6\text{H}_4)\text{PO}(\text{OEt})_2]_2$; PO_3 (---), *cis*- PPh_2M or OPPh_2 (···), *trans*- PPh_2M (—), PPh_2 (—)).

= Et, SiMe_3) groups with surface M–OH groups and by coordination of the phosphoryl groups.^{2,3,23,31,32} The ^{31}P MAS NMR spectra of grafted complexes **1** and **3** (Fig. 4) are qualitatively similar to the spectra obtained for **X5** and **X7** (Fig. 3), respectively.

In both cases, only signals relative to grafted phosphonate groups and phosphine ligands were present, indicating that precipitation of bulk metal phosphonate phases did not occur.² In the case of **G1**, the ^{31}P MAS NMR spectrum can be satisfactorily simulated using two sets of signals: a resonance at 28.4 ppm (phosphonate sites) and a triplet centered at 7.7 ppm with a coupling constant of about 3400 Hz. The resonance at 28.4 ppm corresponds to alkylphosphonate groups bonded to titania.³³ The chemical shift and coupling constant of the triplet are characteristic of phosphine sites complexed by Pt(II) in a *cis* geometry.

In the spectrum of **G2**, the resonance at 11.9 ppm is attributed to arylphosphonate groups bonded to titania.² The resonance at 21.9 ppm may be ascribed to phosphine groups coordinated to Pd atoms in a *trans* geometry (Table 3, entry 9), as in the initial complex **3**. The low field signal at 32.8 ppm can be ascribed to *cis* $\text{Pd}[\text{Ph}_2\text{PC}_6\text{H}_4]_2$ sites, indicating partial isomerization (Table 3, entry 8), and possibly to phosphine oxide groups arising from decomplexation and oxidation (Table 3, entries 7a and 7b). Indeed, a small resonance at –4.1 ppm ascribed to free phosphine groups suggests the occurrence of minor decomplexation. The grafting

Table 6 Carbon content, grafting density and complex loading of the hybrid samples obtained by surface modification of titania with complexes **1** (**G1**) and **3** (**G2**)

Sample	C (%)	Density/ complex nm^{-2}	Loading/mmol complex (mol oxide) $^{-1}$
G1	2.08	0.8	5.6
G2	2.36	0.9	6.0

density (number of complex grafted per nm^2) was estimated from the carbon content and the specific surface area of the samples (Table 6). Similar values were found for **G1** and **G2** (0.8–0.9 complex nm^{-2}). This corresponds to complex loadings of about 6 mmol per mole of TiO_2 (Table 6), much lower than the complex loadings of the xerogels (around 100 mmol per mole of TiO_2 (Table 5)), but the loadings could be easily increased by using metal oxide supports with higher surface area.

Preliminary catalytic tests (Sonogashira reaction)^{34–36} were carried out with complex **3** (homogeneous) and **G2** (heterogeneous). In both cases, the catalytic activity was very low compared to $\text{Cl}_2\text{Pd}(\text{PPh}_3)_2$ or silica-supported catalysts³⁵ and the application of these solids as heterogeneous catalysts was not investigated further.

Conclusions

The results presented here demonstrate that phosphonic esters can provide a valuable alternative to phosphonic acids for the preparation of organic–inorganic hybrids based on metal oxides either by sol–gel processing (bistrimethylsilyl esters) or surface modification (bistrimethylsilyl and diethyl esters). Ester derivatives should prove particularly useful for the synthesis of functional hybrid materials when the functional groups can react with the phosphonic acid groups, or to address problems of solubility.

In this work we used bifunctional phosphine–phosphonate ester derivatives to immobilize Pt or Pd complexes by three different routes. Compared to route 1 (phosphine immobilization followed by complexation), route 2 (direct sol–gel immobilization of preformed complexes) permitted the avoidance of secondary reactions such as phosphine oxidation or formation of phosphonium species. The spectra of the solids obtained by route 3 (grafting of preformed complexes on TiO_2) and route 2 were similar. No uncondensed, “dangling” phosphonic acid groups were detected in the solids prepared by routes 2 and 3, indicating that all the phosphonate groups were bonded to the oxide moiety. Using route 2, solids with high loadings in metal complex but low specific surface area could be obtained. Using route 3, the loadings were lower but the specific surface area can be easily controlled.

References

- P. H. Mutin, G. Guerrero and A. Vioux, *J. Mater. Chem.*, 2005, **15**, 3761.
- G. Guerrero, P. H. Mutin and A. Vioux, *Chem. Mater.*, 2001, **13**, 4367.
- G. Guerrero, P. H. Mutin and A. Vioux, *J. Mater. Chem.*, 2001, **11**, 3161.

- 4 W. Gao, L. Dickinson, C. Grozinger, F. G. Morin and L. Reven, *Langmuir*, 1996, **12**, 6429.
- 5 P. Pechy, F. P. Rotzinger, M. K. Nazeeruddin, O. Kohle, S. M. Zakeeruddin, R. Humphrybaker and M. Gratzel, *J. Chem. Soc., Chem. Commun.*, 1995, 65.
- 6 V. Lafond, C. Gervais, J. Maquet, D. Prochnow, F. Babonneau and P. H. Mutin, *Chem. Mater.*, 2003, **15**, 4098.
- 7 P. Bonhote, J. Moser, R. Humphry-Baker, N. Vlachopoulos, S. Zakeeruddin, L. Walder and M. Gratzel, *J. Am. Chem. Soc.*, 1999, **121**, 1324.
- 8 S. M. Zakeeruddin, M. K. Nazeeruddin, P. Pechy, F. P. Rotzinger, R. Humphrybaker, K. Kalyanasundaram, M. Gratzel, V. Shklover and T. Haibach, *Inorg. Chem.*, 1997, **36**, 5937.
- 9 I. Gillaizeau-Gauthier, F. Odobel, M. Alebbi, R. Argazzi, E. Costa, C. A. Bignozzi, P. Qu and G. J. Meyer, *Inorg. Chem.*, 2001, **40**, 6073.
- 10 G. Will, J. Sotomayor, S. Nagajara Rao and D. Fitzmaurice, *J. Mater. Chem.*, 1999, **9**, 2297.
- 11 J. Sotomayor, G. Will and D. Fitzmaurice, *J. Mater. Chem.*, 2000, **10**, 685.
- 12 C. Maillot, P. Janvier, M.-J. Bertrand, T. Praveen and B. Bujoli, *Eur. J. Org. Chem.*, 2002, 1685.
- 13 T. L. Schull, L. Henley, J. R. Deschamps, R. J. Butcher, D. P. Maher, C. A. Klug, K. Swider-Lyons, W. J. Dressick, B. Bujoli, A. E. Greenwood, L. K. Byington Congiardo and D. A. Knight, *Organometallics*, 2007, **26**, 2272.
- 14 J. Blümel, *Inorg. Chem.*, 1994, **33**, 5050.
- 15 J. Sommer, Y. Yang, D. Rambow and J. Blümel, *Inorg. Chem.*, 2004, **43**, 7561.
- 16 D. G. Hewitt and M. W. Teese, *Aust. J. Chem.*, 1984, **37**, 205.
- 17 P. Machnitzki, T. Nickel, O. Stelzer and C. Lanfgrafe, *Eur. J. Inorg. Chem.*, 1998, 1029.
- 18 W. E. McEwen, A. B. Janes, J. W. Knapczyk, V. L. Kyllingstad, W. I. Shiau, S. Shore and J. H. Smith, *J. Am. Chem. Soc.*, 1978, **100**, 7304.
- 19 T. Hirao, T. Masunaga, Y. Ohshiro and T. Agawa, *Synthesis*, 1981, 56.
- 20 G. Guerrero, P. H. Mutin, F. Dahan and A. Vioux, *J. Organomet. Chem.*, 2002, **649**, 113.
- 21 C. E. McKenna and J. Schmidhauser, *J. Chem. Soc., Chem. Commun.*, 1979, 739.
- 22 G. Guerrero, P. H. Mutin and A. Vioux, *Chem. Mater.*, 2000, **12**, 1268.
- 23 P. H. Mutin, G. Guerrero and A. Vioux, *C. R. Chim.*, 2003, **6**, 1153.
- 24 A. Weigt and S. Bischoff, *Phosphorus, Sulfur Silicon Relat. Elem.*, 1995, **102**, 91.
- 25 G. Guerrero, PhD Thesis, University of Montpellier 2, 2000.
- 26 J.-P. Bezombes, C. Chuit, R. J.-P. Corriu and C. Reyé, *J. Mater. Chem.*, 1998, **8**, 1749.
- 27 D. D. Ellis, G. Harrison, A. G. Orpen, H. Phetmung, J. G. DeVries and H. Oevering, *J. Chem. Soc., Dalton Trans.*, 2000, 671.
- 28 S. Ganguly, J. T. Mague and D. M. Roundhill, *Inorg. Chem.*, 1992, **31**, 3500.
- 29 G. A. Neff, C. J. Page, E. Meintjes, T. Tsuda, W.-C. Pilgrim, N. Roberts and W. W. Warren, *Langmuir*, 1996, **12**, 238.
- 30 T. L. Schull, S. L. Brandow and W. J. Dressick, *Tetrahedron Lett.*, 2001, **42**, 5373.
- 31 R. Frantz, J.-O. Durand, M. Granier and G. F. Lanneau, *Tetrahedron Lett.*, 2004, **45**, 2935.
- 32 D. Villemin, B. Moreau, F. Simeon, G. Maheut, C. Fernandez, V. Montouillout, V. Caignaert and P.-A. Jaffres, *Chem. Commun.*, 2001, 2060.
- 33 S. Pawsey, K. Yach and L. Reven, *Langmuir*, 2002, **18**, 5205.
- 34 A. Corma, C. Gonzalez-Arellano, M. Iglesias, S. Perez-Ferreras and F. Sanchez, *Synlett*, 2007, **11**, 1771.
- 35 E. Tyrrell, A. Al-Saadi and J. Millet, *Synlett*, 2005, **3**, 487.
- 36 T. Posset and J. Blümel, *J. Am. Chem. Soc.*, 2006, **128**, 8394.